

THEORETICAL ANALYSIS OF RESONANT HYPER-RAMAN SCATTERING OF LIGHT BY 2 LO PHONONS IN A CdS CRYSTAL

Ludmila E. Semenova

*Prokhorov General Physics Institute of the Russian Academy of Sciences
Vavilov Street 38, Moscow 119991, Russia*

Corresponding author e-mail: sl@kapella.gpi.ru

Abstract

We theoretically study resonant hyper-Raman scattering of light by 2LO phonons in a CdS crystal with the wurtzite structure. The scattering process involving the two-photon dipole transitions to B and C excitons of the *s*-type is considered. The different sequences of intermediate states are taken into account. It is shown that the inclusion of the possible dipole transitions to the deeper valence band, at certain conditions, can have a noticeable effect on the frequency dependence of the scattering cross section.

Keywords: hyper-Raman scattering, exciton, semiconductor.

1. Introduction

The Raman scattering (RS) cross section is known to significantly increase, when the incident photon energy is close to the band gap E_{cv} , and it becomes possible to detect the high-order scattering processes. The first observations of multiphonon resonant Raman scattering (MPRRS) in CdS were reported more than half a century ago [1–3]. Later, a number of publications was devoted to investigation of MPRRS [4–7]. In particular, experimental studies of MPRRS in CdS have been carried out over the wide energy range [4], and in [5] an investigation of the second-order RS in CdS and ZnO using a tunable exciting light source was reported. Two-phonon resonant RS of light on pure and doped CdS and ZnSe samples was experimentally studied, and the results obtained were analyzed with the use of the exciton model [6]. Klyuchikhin et al. performed experimental and theoretical investigations of MPRRS in a CdS crystal, and, in doing so, RS with creation of up to four longitudinal optical (LO) phonons was observed under excitation below the intrinsic absorption edge [7]. Although hyper-Raman scattering (HRS) of light is a three-photon process, in contrast to RS, the 2LO and 3LO lines were found in the resonant HRS spectra of a CdS crystal [8, 9].

Over the past years, multiphonon RS was reported to be observed in investigations of CdS nanoparticles and the CdS thin films [10–14]. RS up to the third order was found in the study of CdS nanoparticles grown on the surface of ZnO films [10]. In [11], multiphonon RS in the CdS nanocrystals, grown by thermal evaporation techniques, after annealing was reported. In the study of nanostructured CdS thin films, along with RS by 1LO phonons, a smaller intense peak attributed to scattering by 2LO phonons was also observed [12]. The Raman spectra of thin CdS films investigated in [13] contained characteristic CdS modes, their multiphonon combinations, and surface optical modes. Scattering by 1LO and 2LO

phonons was found in the Raman spectroscopy studies of CdS thin films [14]. In investigations of resonant HRS by CdS quantum dots, overtone scattering was observed in hyper-Raman spectra [15].

In [7], in the study of MPRRS in a CdS crystal, an irregular character of the change in the scattering intensity with increase in the number of excited LO phonons was found upon excitation below the absorption edge, and the even-order lines predominated. This feature observed was explained within the framework of the exciton model by various sequences of intermediate states [7]. Therefore, it could be expected that increase in the number of photons involved in the HRS process in comparison with RS will lead to the fact that the lines of the odd orders can dominate in the hyper-Raman spectra [16]. Later, this assumption was confirmed by the observation of resonant HRS by 1 LO and 3 LO phonons in a CdS crystal, while the 2 LO line was not found [8]. However, in the study of HRS in CdS using a tunable laser, an appearance of the 2 LO line in the hyper-Raman spectra upon excitation near a two-photon resonance with the 1s exciton level of the A series was detected, and its intensity grown with a further increase in the incident photon energy [9]. In [17], the observed HRS by 2 LO phonons was explained by the scattering mechanism involving two-photon dipole transitions to B and C excitons of the *s*-type, and the scattering cross section as a function of the incident photon energy was calculated. However, this did not account for the absence of the 2 LO line below the excitonic resonance. The present work is devoted to analysis of resonant HRS of light by 2 LO phonons in a CdS crystal with the wurtzite structure.

This paper is organized as follows.

In Sec. 2, we give the basic formulas for the cross section of resonant HRS by 2 LO phonons. In Sec. 3, a theoretical model of two-phonon HRS in CdS is considered. Section 4 is devoted to the results obtained and their discussion.

2. Basic Formulas

From a microscopic point of view, the Stokes process of HRS of light by 2 LO phonons under the two-photon excitation near the absorption edge of a semiconductor crystal can be described as follows: two incident photons with frequency ω_L , wave vector \mathbf{q}_L , and polarization $\boldsymbol{\varepsilon}_L$ are absorbed, then successive creation of two LO phonons with wave vectors \mathbf{q}_1 and \mathbf{q}_2 occurs, and a scattered light photon ($\omega_S, \mathbf{q}_S, \boldsymbol{\varepsilon}_S$) is emitted. In this case, the laws of conservation of energy and wave vector are fulfilled: $\hbar\omega_S = 2\hbar\omega_L - 2\hbar\omega_{LO}$ and $\mathbf{q}_S = 2\mathbf{q}_L - \mathbf{q}_1 - \mathbf{q}_2$, where ω_{LO} is the LO phonon frequency. In this work, we assume that, in the initial and final states, an electronic system of a semiconductor is in the ground state, and the Hydrogen-like Wannier excitons are its intermediate virtual states in the scattering process. The intra-band Fröhlich mechanism of the exciton–lattice interaction is taken into account. The cross section of two-phonon HRS has the form [17–19]

$$\frac{d\sigma}{d\Omega} = \frac{\hbar e^6 n_S \omega_S^2 (n_{LO} + 1)^2 V N_L}{8\pi^2 m^6 c^4 n_L^3 \omega_L^3} \int |B(\mathbf{q}, 2\mathbf{q}_L - \mathbf{q}_S - \mathbf{q}) + B(2\mathbf{q}_L - \mathbf{q}_S - \mathbf{q}, \mathbf{q})|^2 d\mathbf{q}, \quad (1)$$

where e and m are the charge and the mass of an electron, c is the light speed, n_{LO} is the occupation number for LO phonons, V is the crystal volume, N_L is the density of exciting radiation photons, and n_L and n_S are refractivity coefficients for the frequencies ω_L and ω_S , respectively. Then, $B(\mathbf{q}, \mathbf{q}')$ reads

$$B(\mathbf{q}, \mathbf{q}') = \sum_{\Lambda} \frac{\Xi_{\Lambda}(\mathbf{q}, \mathbf{q}') f_{\Lambda}}{E_{\Lambda}(2\mathbf{q}_L) - 2\hbar\omega_L}, \quad (2)$$

where the sum runs over the intermediate exciton states Λ , to which the energy levels $E_\Lambda(2\mathbf{q}_L)$ correspond. In Eq. (2), f_Λ is given by

$$f_\Lambda = \sum_{\Lambda_1} \frac{\varepsilon_\beta^{(L)} \varepsilon_\alpha^{(L)} \Pi_{\Lambda\Lambda_1}^\beta \Pi_{\Lambda_1 0}^\alpha}{E_{\Lambda_1}(\mathbf{q}_L) - \hbar\omega_L}, \quad (3)$$

where $\Pi_{\Lambda\Lambda_1}^\beta$ and $\Pi_{\Lambda_1 0}^\alpha$ describe the transitions between the exciton states and between the ground and exciton states, respectively [17, 20–22]. Then, $\Xi_\Lambda(\mathbf{q}, \mathbf{q}')$ has the form

$$\Xi_\Lambda(\mathbf{q}, \mathbf{q}') = \sum_{\Lambda_2, \Lambda_3} \frac{\varepsilon_\gamma^{(S)} \Pi_{0\Lambda_3}^\gamma U_{\Lambda_3\Lambda_2}(\mathbf{q}) U_{\Lambda_2\Lambda}(\mathbf{q}')}{[E_{\Lambda_3}(\mathbf{q}_S) - \hbar\omega_S][E_{\Lambda_2}(\mathbf{q}_S + \mathbf{q}) + \hbar\omega_{LO} - 2\hbar\omega_L]}, \quad (4)$$

where $U_{\Lambda'\Lambda}(\mathbf{q})$ describes the transitions between the exciton states due to the Fröhlich interaction [17, 23]. Further, we neglect the photon wave vectors, owing to their smallness.

3. Theoretical Model

In [9], the resonant HRS by 2LO phonons in CdS was observed for the 90° scattering geometry, in which the exciting radiation was directed along the optical axis. As in [17], in the present paper, we consider the two-phonon HRS process involving two-photon dipole transitions to B and C excitons of the s -type of the Γ_1 symmetry for this scattering configuration. But, in doing so, the valence band wave functions obtained in the work by Gutsche and Jahne [24] are taken into account. In compliance with it, in the semiconductors with the wurtzite structure, in the center of the Brillouin zone, the spin-orbit interaction leads to the fact that, in the B and C subbands, the wave functions u_{1v} and u_{5v} (u_{5v}^*) transforming according to the irreducible representations Γ_1 and Γ_5 mix, and, in the A subband and the deeper valence band v' of the symmetry Γ_9 , a mixing of the wave functions u_{6v} (u_{6v}^*) belonging to the representation Γ_6 and u_{5v} (u_{5v}^*) occurs. Moreover, the subband A is mostly determined by u_{5v} (u_{5v}^*) with a small addition of u_{6v} (u_{6v}^*), and, in the band v' (Γ_9), on the contrary, the wave functions u_{6v} (u_{6v}^*) prevail. The appropriate wave functions were given in [25].

At first sight, the hyper-Raman process considered is similar to two-LO-phonon RS, which has been theoretically studied, within the framework of the exciton model, in several papers [26, 27]. In particular, by using the Green's function method [28], the expressions that make it possible to account for the contributions of the sequences of intermediate exciton states $s - s - s$ and $s - p - s$ to RS were obtained [27]. In the present work, both the transitions between s and p -excitons and the transitions between s -excitons, due to the Fröhlich interaction, are also taken into account. Thus, $\Xi_\Lambda(\mathbf{q}, \mathbf{q}')$ for B and C exciton contributions to HRS can be written as

$$\Xi_\xi^B(\mathbf{q}, \mathbf{q}') = \frac{2}{\sqrt{2}} \varepsilon_z^{(S)} P_{vc}^{\parallel} q_{7v} \gamma_F^2 A_\xi^B(\mathbf{q}, \mathbf{q}', E_{cv}^B, R_B, \alpha_e^B, \alpha_h^B) \quad (5)$$

and

$$\Xi_\xi^C(\mathbf{q}, \mathbf{q}') = \frac{-2}{\sqrt{2}} \varepsilon_z^{(S)} P_{vc}^{\parallel} \sqrt{1 - q_{7v}^2} \gamma_F^2 A_\xi^C(\mathbf{q}, \mathbf{q}', E_{cv}^C, R_C, \alpha_e^C, \alpha_h^C), \quad (6)$$

where $\gamma_F = \sqrt{2\pi\hbar\omega_{LO}e^2(\varepsilon_\infty^{-1} - \varepsilon_0^{-1})}$, ε_∞ and ε_0 are the optical and static dielectric constants, $E_{cv}^B = E_{cv} + \Delta_{AB}$, $E_{cv}^C = E_{cv} + \Delta_{AC}$, Δ_{AB} (Δ_{AC}) is the energy splitting between the subbands A and B (C),

$\alpha_e^{B(C)} = m_{B(C)}^*/(m_e^* + m_{B(C)}^*)$, $\alpha_h^{B(C)} = m_e^*/(m_e^* + m_{B(C)}^*)$, m_e^* and $m_{B(C)}^*$ are the effective masses of an electron in the conduction band and a hole in the B (C) subband. The matrix element P_{vc}^{\parallel} is given by $P_{vc}^{\parallel} = \langle u_{1v} | \hat{p}_z | u_{1c} \rangle$, where $\hat{p}_\alpha = -i\hbar \frac{\partial}{\partial r_\alpha}$, u_{1c} is the wave function related to the lowest conduction band and transforming according to the irreducible representation Γ_1 . Then, q_{7v}^2 determines the fraction of u_{1v} in the B subband, and $A_\xi^{B(C)}(\mathbf{q}, \mathbf{q}', E, R, \alpha_e, \alpha_h)$ has the form

$$A_\xi^{B(C)}(\mathbf{q}, \mathbf{q}', E, R, \alpha_e, \alpha_h) = \sum_{\xi'} \sum_{\ell=0}^1 \sum_{m=-\ell}^{\ell} \left[\sum_{\xi''} \frac{\chi_{B(C)}^{(\xi''00)}(0) \langle \chi_{B(C)}^{(\xi''00)} | iq^{-1}(e^{-i\alpha_e \mathbf{q} \cdot \mathbf{r}} - e^{i\alpha_h \mathbf{q} \cdot \mathbf{r}}) | \chi_{B(C)}^{(\xi' \ell m)} \rangle}{E - R\Theta_{\xi''}^{-2} - \hbar\omega_S} \right] \times \frac{\langle \chi_{B(C)}^{(\xi' \ell m)} | iq'^{-1}(e^{-i\alpha_e \mathbf{q}' \cdot \mathbf{r}} - e^{i\alpha_h \mathbf{q}' \cdot \mathbf{r}}) | \chi_{B(C)}^{(\xi 00)} \rangle}{E - R\Theta_{\xi'}^{-2} + \frac{\hbar^2 q^2}{2(m_e^* + m_{B(C)}^*)} + \hbar\omega_{LO} - 2\hbar\omega_L}, \quad (7)$$

where $\chi_{cv}^{(\xi \ell m)}(\mathbf{r})$ is the wave function of the relative electron–hole motion, and $(\xi \ell m)$ is the set of the quantum numbers corresponding to it. The indices B and C related to the exciton Rydberg $R_{B(C)}$ and the wave functions $\chi_{B(C)}^{(\xi \ell m)}(\mathbf{r})$ indicate their connection with the appropriate excitonic series. Here, the following notion is used for Θ_ξ : $\Theta_n = n$ ($\xi = n$) for the discrete spectrum and $\Theta_k = i/k$ ($\xi = k$) for the continuous spectrum.

For the excitation range, considered in this work, the frequency of scattered radiation is smaller than the one of the exciton resonance, $\hbar\omega_S < E_{cv}^B - R_B$. Therefore, for the sums over ξ'' in Eq. (7), we adopt the expressions obtained by the use of the Green's function method [28] in [27]. The matrix elements $\langle \chi_{cv}^{(\xi' \ell m)} | iq^{-1}(e^{-i\alpha_e \mathbf{q} \cdot \mathbf{r}} - e^{i\alpha_h \mathbf{q} \cdot \mathbf{r}}) | \chi_{cv}^{(\xi 00)} \rangle$ ($\ell = 0$ and 1) for the transitions between discrete states and the transitions between discrete and continuous states were obtained in [29, 30]. To calculate the matrix elements for the transitions between states of the continuous spectrum, we take the wave functions $\tilde{\chi}_{cv}^{(k \ell m)}(\mathbf{r}) = Y_{\ell m}(\theta, \phi) \tilde{R}_{k\ell}^{cv}(r)$, where $Y_{\ell m}(\theta, \phi)$ are the spherical functions; the radial functions $\tilde{R}_{k\ell}^{cv}(r)$ are adopted in the approximation of the unbound electron–hole pairs [31]. Using the expansion of a plane wave in the spherical functions [31], it is not difficult to reduce these matrix elements to the Bessel functions integrals given in [32]. In this case, when summing over ξ'' , we apply the Green's function method [28], by analogy with the approach used in [27], but we perform the calculations for $\tilde{\chi}_{cv}^{(k' \ell m)}(\mathbf{r})$ instead of $\chi_{cv}^{(\xi' \ell m)}(\mathbf{r})$.

However, in contrast to RS, the two-phonon HRS process considered here involves two-photon dipole transitions to s -exciton states. As is known [21, 33, 34], a two-photon dipole transition to an s -exciton composed of an electron from the lowest conduction band c and a hole from the top valence band v can occur via an intermediate p -exciton state belonging to the same pair of bands, as well as an s -exciton state formed by an electron from the higher-lying conduction band and a hole from the valence band v or an electron from the conduction band c and a hole from the deeper valence band. According to the selection rules, the two-photon transitions to B and C excitons (Γ_1) are possible through the intermediate s -exciton states associated with both the higher-lying conduction band c' ($\Gamma_9, \Gamma_7, \Gamma_7$) [35] and the deeper valence band v' (Γ_9). In the latter case, this is eventual only due to the addition of the wave functions u_{5v} (u_{5v}^*) in the band v' . When considering within the framework of the two-band model, the two-photon transition to an s -exciton includes the weakly forbidden dipole transition to an exciton of the p -type. Its

matrix element depends on $M_{jcjv}^{\beta\alpha}$ [20, 34],

$$M_{jcjv}^{\beta\alpha} = \frac{1}{m} \sum'_n \left(\frac{\pi_{jc'n}^\beta \pi_{njv}^\alpha}{E_{jc'n}} + \frac{\pi_{jc'n}^\alpha \pi_{njv}^\beta}{E_{jv'n}} \right), \quad (8)$$

where j_c and j_v denote the states in the bands c and v , respectively, $E_{jj'}$ is the energy difference between the bands, $\pi_{jj'}$ is the inter-band matrix element of the momentum operator. In Eq. (8), the \sum'_n means that the sum is over all bands, except c and v . In this study, when calculating $M_{jcjv}^{\beta\alpha}$, we take into account only the contributions of the bands c' and v' . The known band structure of the crystal and the selection rules made it possible to determine the matrix elements of the necessary inter-band dipole transitions.

Since the frequency of the exciting radiation is far from the resonant region, the Green's function method [28] can be used for summation over the intermediate exciton states Λ_1 in Eq. (3). Thus, taking into account the results obtained in [21, 22, 34], we obtain f_Λ for B and C excitons as follows:

$$\begin{aligned} f_\xi^B = & \frac{2}{\sqrt{2}} \left(\varepsilon_x^{(L)} \varepsilon_x^{(L)} + \varepsilon_y^{(L)} \varepsilon_y^{(L)} \right) \chi_B^{(\xi 00)}(0)^* \left\{ 2q_{7v} P_{cc'}^\perp \tilde{P}_{c'v}^\perp \left[\frac{J_1(\theta_\xi, \varkappa_L(E_{c'v}^B), \tilde{a}_B/a_B)}{E_{c'v}^B - \hbar\omega_L} \right. \right. \\ & - \frac{\mu_B}{\mu_B^\perp} \left(\frac{1}{E_{c'c}} + \frac{1}{E_{c'v}^B} \right) J_2(\Theta_\xi, \varkappa_L(E_{cv}^B)) \left. \left. \right] - q_{9v} P_{cv}^\perp \left(\sqrt{1 - q_{7v}^2} \sqrt{1 - q_{9v}^2} P_{v'v}^\perp + q_{7v} q_{9v} \tilde{P}_{v'v}^\perp \right) \right. \\ & \left. \times \left[\frac{J_1(\theta_\xi, \varkappa_L(E_{cv'}), a_{cv'}/a_B)}{E_{cv'} - \hbar\omega_L} - \frac{\mu_B}{\mu_B^\perp} \left(\frac{1}{E_{cv'}} + \frac{1}{E_{vv'} - \Delta_{AB}} \right) J_2(\theta_\xi, \varkappa_L(E_{cv}^B)) \right] \right\} \quad (9) \end{aligned}$$

and

$$\begin{aligned} f_\xi^C = & -\frac{2}{\sqrt{2}} \left(\varepsilon_x^{(L)} \varepsilon_x^{(L)} + \varepsilon_y^{(L)} \varepsilon_y^{(L)} \right) \chi_C^{(\xi 00)}(0)^* \left\{ 2\sqrt{1 - q_{7v}^2} P_{cc'}^\perp \tilde{P}_{c'v}^\perp \left[\frac{J_1(\theta_\xi, \varkappa_L(E_{c'v}^C), \tilde{a}_C/a_C)}{E_{c'v}^C - \hbar\omega_L} \right. \right. \\ & - \frac{\mu_C}{\mu_C^\perp} \left(\frac{1}{E_{c'c}} + \frac{1}{E_{c'v}^C} \right) J_2(\Theta_\xi, \varkappa_L(E_{cv}^C)) \left. \left. \right] + q_{9v} P_{cv}^\perp \left(q_{7v} \sqrt{1 - q_{9v}^2} P_{v'v}^\perp - q_{9v} \sqrt{1 - q_{7v}^2} \tilde{P}_{v'v}^\perp \right) \right. \\ & \left. \times \left[\frac{J_1(\theta_\xi, \varkappa_L(E_{cv'}), a_{cv'}/a_C)}{E_{cv'} - \hbar\omega_L} - \frac{\mu_C}{\mu_C^\perp} \left(\frac{1}{E_{cv'}} + \frac{1}{E_{vv'} - \Delta_{AC}} \right) J_2(\theta_\xi, \varkappa_L(E_{cv}^C)) \right] \right\}, \quad (10) \end{aligned}$$

where $E_{c'v}^B = E_{c'c} + E_{cv}^B$, $E_{c'v}^C = E_{c'c} + E_{cv}^C$, $\varkappa_L(E_{cv}) = \sqrt{R_{cv}/(E_{cv} - \hbar\omega_L)}$, and q_{9v}^2 defines a part of u_{5v} (u_{5v}^*) in the band v' (Γ_9). Also, R_{cv} , μ_{cv} , and a_{cv} are the excitonic Rydberg, the effective mass, and the Bohr radius of the exciton composed of an electron from the conduction band c and a hole from the valence band v ; the indices B and C related to $\mu_{B(C)}$, and $a_{B(C)}$ indicate belonging to the appropriate excitonic series. Here, \tilde{a}_B (\tilde{a}_C) is the Bohr radius of the exciton formed by an electron from the conduction band c' and a hole from the subband B (C). Matrix elements of the dipole transitions are defined as follows: $P_{cv}^\perp = \langle u_{1c} | \hat{p}_x | u_{5v} \rangle$, $P_{cc'}^\perp = \langle u_{1c} | \hat{p}_x | u_{5c'} \rangle$, $\tilde{P}_{c'v}^\perp = \langle u_{5c'} | \hat{p}_x | u_{1v} \rangle$, $P_{v'v}^\perp = \langle u_{6v} | \hat{p}_x | u_{5v} \rangle$, and $\tilde{P}_{v'v}^\perp = \langle u_{5v} | \hat{p}_x | u_{1v} \rangle$, where $u_{5c'}$ is the wave function belonging to the higher-lying conduction band c' and transforming over the irreducible representation Γ_5 .

The function $J_2(\Theta_\xi, \varkappa_L)$ is given in [22], and $J_1(\Theta_\xi, \varkappa_L, b)$ can be approximated by $[1 - (\varkappa_L b / \Theta_\xi)^2]^{-1}$ since, under the conditions considered, $\varkappa_L \ll 1$ [21, 22]. In this case, $J_1(\Theta_\xi, \varkappa_L(E_{c'v'}), a_{c'v'}/a_{cv})$ can be expressed as $J_1(\Theta_\xi, \varkappa_L(E_{c'v'}), a_{c'v'}/a_{cv}) \approx [1 - R_{cv}(E_{c'v'} - \hbar\omega_L)^{-1} \Theta_\xi^{-2} \tilde{b}]^{-1}$, where $\tilde{b} = \mu_{cv}/\mu_{c'v'}$. Further, in calculations, we assume that $\tilde{b} = 1$.

As noted above, the matrix elements for the transitions between exciton states of the continuous spectrum, owing to the Fröhlich interaction, are considered in the approximation of the unbound electron–hole pairs. In this case, in the corresponding expressions for f_ξ^B and f_ξ^C , it is also necessary to take $\tilde{\chi}_{cv}^{(k00)}(0)$ instead $\tilde{\chi}_{cv}^{(\xi 00)}(0)$, when calculating $B(\mathbf{q}, \mathbf{q}')$. In so doing, $J_2(\Theta_\xi, \varkappa_L)$ is replaced by the function $\tilde{J}_2(k, \varkappa_L)$, which is derived similarly to $J_2(\Theta_\xi, \varkappa_L)$ but for $\tilde{\chi}_{cv}^{(k00)}(\mathbf{r})$.

Equations (9) and (10) can be simplified, using the approach applied in [36], i.e., assuming that $\sqrt{1 - q_{9v}^2} |P_{v'v}^\perp| \gg |q_{9v} \tilde{P}_{v'v}^\perp|$. In this case, if the notation $D = q_{9v} q_{7v} \sqrt{1 - q_{9v}^2} \sqrt{1 - q_{7v}^2} (P_{cv}^\perp P_{v'v}^\perp) / (P_{cc'}^\perp \tilde{P}_{c'v}^\perp)$ is adopted [36], then the contribution of the hyper-Raman process involving in the two-photon transitions to B excitons, and $B(\mathbf{q}, \mathbf{q}')$ can be presented as $B_B(\mathbf{q}, \mathbf{q}') \cong B_B^{(c')}(\mathbf{q}, \mathbf{q}') - DB_B^{(v')}(\mathbf{q}, \mathbf{q}')$. The contribution of the scattering process with a participation of C excitons can be written as $B_C(\mathbf{q}, \mathbf{q}') \cong B_C^{(c')}(\mathbf{q}, \mathbf{q}') + DB_C^{(v')}(\mathbf{q}, \mathbf{q}')$. Here, $B_{B(C)}^{(c')}(\mathbf{q}, \mathbf{q}')$ and $B_{B(C)}^{(v')}(\mathbf{q}, \mathbf{q}')$ are associated with the transitions to the higher-lying conduction band c' and the deeper valence band v' , respectively.

4. Results and Discussion

We calculate the cross section of HRS by 2 LO phonons in CdS as a function of the doubled energy of incident photons. Since q_{9v} and the matrix elements of the dipole transitions to the bands c' and v' are unknown, we carry out the computations for various values of D . In calculations, the following crystal parameters are used: $E_{cv} = 2.578$ eV, $\Delta_{AB} = 0.015$ eV, $\Delta_{AC} = 0.078$ eV [37], $R_B = 0.028$ eV, $R_C = 0.026$ eV [38], $E_{c'c} = 5.4$ eV, $E_{vv'} = 0.6$ eV [39], and $\hbar\omega_{LO} = 0.038$ eV [40]. When computing, we adopt the electron and hole effective masses given in [37], but we neglect their anisotropy and use the scalar values $m_e^* \approx 0.205 m$, $m_B^* \approx 0.8 m$, and $m_C^* \approx 0.85 m$. For q_{7v}^2 , the expression $(1 - q_{7v}^2) / q_{7v}^2 \approx 0.9$ was obtained in [36], with the use of the known oscillator strengths of the transitions to the 1s exciton states of the B and C series [41]. The Bohr radii of the B and C excitons were assumed to be the same.

As already indicated above, the scattering process considered here involves the two-photon transitions to B and C exciton states. For these states, the lifetime broadenings Γ were taken into account; for discrete s-excitons of the B and C series, the values $\Gamma_B = 0.006$ eV and $\Gamma_C = 0.016$ eV were considered [41]. In the case of continuous states, Γ_B and Γ_C were assumed to be equal to the corresponding exciton Rydbergs.

It should be noted that, in [36], the one-phonon HRS cross section as a function of the doubled energy of incident photons was calculated for several values of D . But in the present paper, a situation is different, because the phonons with various wave vectors give a contribution to the second-order HRS.

In Fig. 1, we present the two-phonon HRS cross section calculated for several values of D versus $2\hbar\omega_L$. As one can see, the inclusion of the possible dipole transitions to the deeper valence band v' (Γ_9) leads to increase in the HRS cross section for $D < 0$ and gives rise to its decrease, when $D > 0$. However, a more interesting behavior is shown by the frequency dependence of $\frac{d\sigma}{d\Omega}$ at $D = 0.8$ and 1. In these cases, with increase in the doubled energy of incident photons, the scattering cross section first changes little, and then its fast growth begins.

Such a behavior of the frequency dependence of the cross section for $D > 0$ can be explained as follows. In the considered excitation range, the hyper-Raman process involving the two-photon transitions to B excitons prevails when $D = 0$. For small values of $D > 0$, its contribution to HRS decreases, in contrast to the one associated with C excitons. As D increases, an appearance of $B_B(\mathbf{q}, \mathbf{q}')$ opposite in sign

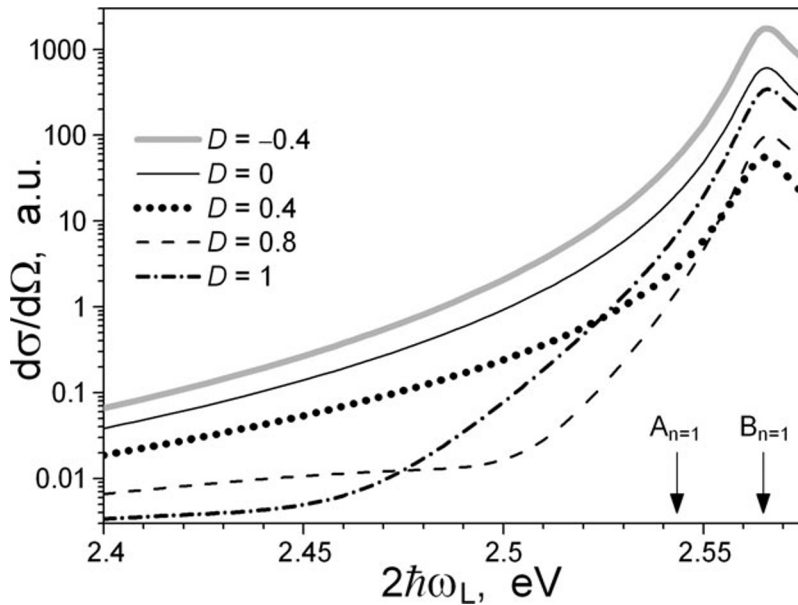


Fig. 1. The two-phonon HRS cross section calculated for several values of D as a function of the doubled energy of incident photons. The arrows show the positions of the $1s$ exciton levels of the A ($A_{n=1}$) and B ($B_{n=1}$) series.

to $B_C(\mathbf{q}, \mathbf{q}')$ begins. At the same time, as the two-photon resonance with the $1s$ exciton level of the B series is approached, the relative contribution of the scattering process associated with B excitons rapidly increases.

Unfortunately, it is difficult to compare the results of the performed calculations with the experimental ones, since there is not the necessary data on the intensity of the observed 2LO line. In the experimental studies, using a tunable laser [9], the intensity of HRS by 1LO phonons increased by more than two orders of magnitude, when the doubled energy of incident photons changed within the range from 2.39 to 2.53 eV. At the exciting radiation wavelength $\lambda_L = 9760 \text{ \AA}$, i.e., near the two-photon resonance with the $1s$ exciton level of the A series, its decrease due to the attenuation of scattered light near the absorption edge was observed, but an appearance of the 2LO line in the hyper-Raman spectra was found, and its intensity grew with a further increase of $2\hbar\omega_L$ [9]. It is most likely that the absence of the 2LO line in the scattering spectra, under excitation below the two-photon resonance with the lowest exciton level, is due to the fact that its intensity decreases rapidly with distance from the resonance. As the results of the performed calculations showed, when varying the doubled energy of incident photons in the range from 2.4 to 2.541 eV, the cross section of HRS by 2LO phonons increases by about 400 times at $D = 0$ and by about 1500 times at $D = 1$; moreover, in the latter case, its growth by about 800 times falls in the range of 2.46–2.541 eV. Thus, the fact that the 2LO line was detected near the two-photon resonance and was not seen in the scattering spectra below it [9] could be due to the behavior of the frequency dependence of the scattering cross section, which is similar to that calculated for $D = 1$.

5. Conclusions

We analyzed the resonant HRS of light by 2LO phonons in wurtzite CdS. In doing so, the hyper-Raman process involving two-photon dipole transitions to s -excitons of the B and C series was considered. The influence of the possible dipole transitions to the deeper valence band (Γ_9) on the frequency dependence of the scattering cross section was investigated. We showed that, under certain conditions, taking

into account these transitions could lead to the fact that a rapid growth of $\frac{d\sigma}{d\Omega}$ began somewhat below the two-photon resonance with the lowest exciton level. It is possible that the previously observed appearance of the 2LO line in the HRS spectra, when $2\hbar\omega_L$ is close to the energy of the $1s$ exciton state of the A series and its absence under two-photon excitation below the region of excitonic resonances [9] are due to such a behavior of the scattering cross section.

References

1. R. C. C. Leite and S. P. S. Porto, *Phys. Rev. Lett.*, **17**, 10 (1966).
2. R. C. C. Leite, J. F. Scott, and T. C. Damen, *Phys. Rev. Lett.*, **22**, 780 (1969).
3. J. F. Scott, R. C. C. Leite, and T. C. Damen, *Phys. Rev.*, **188**, 1285 (1969).
4. R. H. Callender, S. S. Sussman, M. Selders, and R. K. Chang, *Phys. Rev. B*, **7**, 3788 (1973).
5. Y. Oka and T. Kushida, *J. Phys. Soc. Jpn.*, **33**, 1372 (1972).
6. P. Verma, S. Anand, and K. P. Jain, *Physica B*, **271**, 1 (1999).
7. A. A. Klyuchikhin, S. A. Permogorov, and A. N. Reznitskii, *Sov. Phys. JETP*, **44**, 1176 (1976).
8. L. E. Zubkova, K. K. Ondriash, Yu. N. Polivanov, and K. A. Prokhorov, *JETP Lett.*, **57**, 348 (1993).
9. V. A. Maslov, K. K. Ondriash, Yu. N. Polivanov, et al., *Laser Phys.*, **6**, 132 (1996).
10. A. V. Kozytskiy, O. L. Stroyuk, S. Ya. Kuchmiy, et al., *Thin Solid Films*, **562**, 56 (2014).
11. S. Farid, M. A. Stroschio, and M. Dutta, *Superlattices Microstruct.*, **115**, 204 (2018).
12. M. Waldiya, R. Narasimman, D. Bhagat, et al., *Mater. Chem. Phys.*, **226**, 26 (2019).
13. J. Trajić, M. Gilić, N. Romčević, et al., *Sci. Sintering*, **47**, 145 (2015).
14. A. Ashok, G. Regmi, A. Romero-Núñez, et al., *J. Mater. Sci.: Mater. Electron.*, **31**, 7499 (2020).
15. R. Tan, D. F. Kelley, and A. M. Kelley, *J. Phys. Chem. C*, **123**, 16400 (2019).
16. R. Sh. Sayakhov, *Trudy IOFAN*, **2**, 56 (1986) [in Russian].
17. L. E. Semenova and K. A. Prokhorov, *Laser Phys. Lett.*, **2**, 262 (2005).
18. L. E. Semenova, G. Yu. Nikolaeva, P. P. Pashinin, and K. A. Prokhorov, *Laser Phys.*, **19**, 776 (2009).
19. L. Semenova and K. Prokhorov, *Phys. Status Solidi C*, **1**, 3118 (2004).
20. M. M. Denisov and V. P. Makarov, *Phys. Status Solidi B*, **56**, 9 (1973).
21. K. C. Rustagi, F. Pradere and A. Mysyrowicz, *Phys. Rev. B*, **8**, 2721 (1973).
22. L. E. Semenova and K. A. Prokhorov, *JETP*, **96**, 922 (2003).
23. R. M. Martin, *Phys. Rev. B*, **4**, 3676 (1971).
24. E. Gutsche and E. Jahne, *Phys. Status Solidi*, **19**, 823 (1967).
25. L. C. Lew Yan Voon, M. Willatzen, M. Cardona, and N. E. Christensen, *Phys. Rev. B*, **53**, 10703 (1996).
26. A. García-Cristóbal, A. Cantarero, C. Trallero-Giner, and M. Cardona, *Phys. Rev. B*, **49**, 13430 (1994).
27. L. E. Semenova and K. A. Prokhorov, *J. Raman Spectrosc.*, **32**, 942 (2001).
28. L. Hostler, *J. Math. Phys.*, **5**, 591 (1964).
29. L. E. Semenova and K. A. Prokhorov, *Proc. SPIE*, **4748**, 275 (2002).
30. C. Trallero-Giner, A. Cantarero, and M. Cardona, *Phys. Rev. B*, **40**, 4030 (1989).
31. L. D. Landau and E. M. Lifshitz, *Course of Theoretical Physics*, vol. 3: Quantum Mechanics: Non-relativistic Theory, Pergamon, New York (1977).
32. A. P. Prudnikov, Yu. A. Brychkov, and O. I. Marichev, *Integrals and Series, Special Functions*, Nauka, Moscow (1983) [in Russian]; [English translation: Gordon and Breach Sci. Publ., New York (1986)].
33. R. Loudon, *Proc. Phys. Soc.*, **80**, 952 (1962).
34. G. D. Mahan, *Phys. Rev.*, **170**, 825 (1968).
35. M. Cardona and G. Harbeke, *Phys. Rev.*, **137**, A1467 (1965).
36. L. E. Semenova, *Laser Phys.*, **32**, 084004 (2022).
37. B. A. Nguyen, V. H. Nguyen, T. T. Nguyen, and A. V. Nguyen, *Phys. Rev. B*, **25**, 4075 (1982).

38. D. C. Reynolds, "Excitons in II-VI compounds" in *Optical Properties of Solids*, Plenum Press, New York (1969), p. 239.
39. A. Kobayashi, O. F. Sankey, S. M. Volz, and J. D. Dow, *Phys. Rev. B*, **28**, 935 (1983).
40. *Physics and Chemistry of II-VI Compounds*, M. Aven and J. S. Prener (Eds.), North-Holland, Amsterdam (1967); [Russian translation: Mir, Moscow (1970)].
41. V. V. Sobolev, *Bands and Excitons of the A^{II}B^{VI} Group Compounds*, Shtiintsa, Chisinau (1980) [in Russian].